

Black holes in galactic centers: quasinormal ringing, grey-body factors and Unruh temperature

R. A. Konoplya,^{*†}

^{*}Research Centre for Theoretical Physics and Astrophysics,
Institute of Physics, Silesian University in Opava,
Bezručovo náměstí 13, CZ-74601 Opava, Czech Republic

[†]Peoples Friendship University of Russia (RUDN University),
6 Miklukho-Maklaya Street, Moscow 117198, Russian Federation

E-mail: roman.konoplya@gmail.com

Abstract. Recently, Cardoso et al. [1] found an exact black hole solution describing the black hole immersed in a galactic-like distribution of matter. There, the properties of gravitational radiation were studied. Here we continue analysis of properties of this geometry via consideration of electromagnetic radiation. We calculate quasinormal modes, asymptotic tails and grey-body factors for electromagnetic radiation. In addition, we discuss the Unruh temperature for this spacetime. Estimations made in the regime which is best fitting the galaxies behavior show that influence of the environment on classical and quantum radiation around such black holes must be relatively small.

Contents

1	Introduction	1
2	Master wave equations	2
3	Quasinormal modes and late time tails	2
4	Grey-body factors	4
5	Unruh temperature	6
6	Conclusions	7

1 Introduction

Perturbations, quasinormal modes, radiation effects particle motion and thermodynamics around black holes immersed in astrophysical environment have been actively studied in the literature (see for instance [2–6] and references therein). In this context recent work by Cardoso et. al. [1] suggested an interesting black hole solution which describes a black hole immersed in the distribution of matter (with anisotropic pressure) which meets the observations of galaxies. The gravitational perturbations as well as basic aspects of particle motion were considered in [1]. Here we will study propagation of the electromagnetic perturbations, which includes quasinormal modes, late time tails and scattering properties. In addition, we will consider the Unruh temperature for a given spacetime, which is a characteristic of the surface gravity at a given point in space.

In [1] the Hernquist-type density distribution [7] was used for modelling the Sérsic profiles that are observed in bulges and elliptical galaxies:

$$\rho = \frac{Ma_0}{2\pi r(r+a_0)^3}, \quad (1.1)$$

where M is the total mass of the “halo” and a_0 a typical lengthscale of the galaxy under consideration. The metric has the following general form:

$$ds^2 = -f dt^2 + \frac{dr^2}{1 - 2m(r)/r} + r^2 d\Omega^2, \quad (1.2)$$

The matter distribution suggested by the Hernquist profile (1.1) implies the following mass function:

$$m(r) = M_{\text{BH}} + \frac{Mr^2}{(a_0 + r)^2} \left(1 - \frac{2M_{\text{BH}}}{r}\right)^2, \quad (1.3)$$

which is compatible with the asymptotic flatness ($f \rightarrow 1$ at large r). At small distances the above profile describes a source of mass M_{BH} which goes over to the Hernquist distribu-

tion (1.1) at large scales. The metric function $f(r)$ has the form

$$f = \left(1 - \frac{2M_{\text{BH}}}{r}\right) e^{\Upsilon}, \quad (1.4)$$

$$\Upsilon = -\pi\sqrt{\frac{M}{\xi}} + 2\sqrt{\frac{M}{\xi}} \arctan \frac{r + a_0 - M}{\sqrt{M\xi}}, \quad (1.5)$$

$$\xi = 2a_0 - M + 4M_{\text{BH}}. \quad (1.6)$$

The best fit of galaxies' observations corresponds to $a_0 \gtrsim 10^4 M$. The matter density is

$$4\pi\rho = \frac{m'}{r^2} = \frac{2M(a_0 + 2M_{\text{BH}})(1 - 2M_{\text{BH}}/r)}{r(r + a_0)^3}. \quad (1.7)$$

At large distances and for $a_0 \gg M_{\text{BH}}$, this density profile is that of Hernquist. The event horizon is located then at $r = 2M_{\text{BH}}$. The ADM mass is $M + M_{\text{BH}}$.

2 Master wave equations

The general covariant equations for the electromagnetic field A_μ have the form:

$$\frac{1}{\sqrt{-g}} \partial_\mu (F_{\rho\sigma} g^{\rho\nu} g^{\sigma\mu} \sqrt{-g}) = 0, \quad (2.1a)$$

$$(2.1b)$$

where $F_{\mu\nu} = \partial_\mu A_\nu - \partial_\nu A_\mu$. After separation of the variables Eqs. (2.1) take the following Schrödinger-like form (see, for instance, [8, 9])

$$\frac{\partial^2 \Psi}{\partial t^2} - \frac{\partial^2 \Psi}{\partial r_*^2} = V(r) \Psi, \quad (2.2)$$

where the ‘‘tortoise coordinate’’ r_* is defined by the relation

$$dr_* = \frac{dr}{\sqrt{f(r)(1 - (2m(r)/r))}}. \quad (2.3)$$

The effective potentials for the electromagnetic field is

$$V(r) = f(r) \frac{\ell(\ell + 1)}{r^2}, \quad (2.4)$$

where $\ell = 0, 1, 2, \dots$ are the multipole numbers. In the astrophysically motivated range of parameters the effective potentials have the form of the positive definite potential barriers.

3 Quasinormal modes and late time tails

Quasinormal modes ω_n are frequencies corresponding to solutions of the master wave equation (2.2) with the requirement of the purely outgoing waves at infinities and at the event horizon:

$$\Psi \propto e^{-i\omega t \pm i\omega r_*}, \quad r_* \rightarrow \pm\infty. \quad (3.1)$$

a_0	$M = 10M_{BH}$	$M = 20M_{BH}$
10^4M	0.496459-0.184975 i	0.496410-0.184956 i
$5000M$	0.496261-0.184901 i	0.496013-0.184804 i
$1000M$	0.496013-0.184808 i	0.495517-0.184624 i
$200M$	0.494033-0.184069 i	0.491560-0.183146 i
$100M$	0.491568-0.183146 i	0.486644-0.181305 i
$40M$	0.484247-0.180386 i	0.472086-0.175820 i
$20M$	0.472278-0.175819 i	0.448451-0.166809 i
$10M$	0.449182-0.166818 i	0.403434-0.149339 i

Table 1. Fundamental ($n = 0, \ell = 1$) quasinormal mode of the electromagnetic field as a function of a_0 calculated by the higher order WKB approach. The corresponding Schwarzschild mode is $\omega = 0.496527 - 0.184975i$; $M_{BH} = 1/2$.

a_0	$M = 10M_{BH}$	$M = 20M_{BH}$
10^4M	0.915100-0.189992 i	0.915009-0.189973 i
$5000M$	0.914734-0.189916 i	0.914277-0.189821 i
$1000M$	0.914277-0.189821 i	0.913362-0.189631 i
$200M$	0.910626-0.189061 i	0.906069-0.188114 i
$100M$	0.906083-0.188114 i	0.897004-0.186223 i
$40M$	0.89258-0.1852804 i	0.870156-0.180591 i
$20M$	0.870491-0.180593 i	0.826537-0.171344 i
$10M$	0.827812-0.171363 i	0.743373-0.153426 i

Table 2. Fundamental ($n = 0, \ell = 2$) quasinormal mode of the electromagnetic field as a function of a_0 calculated by the higher order WKB approach. The corresponding Schwarzschild mode is $\omega = 0.915191 - 0.190009i$; $M_{BH} = 1/2$.

In order to find dominant quasinormal modes we will use the two methods: the time-domain integration method [10] and the semi-analytic WKB method [11–14].

In the time domain, we can integrate the wavelike equation (2.2) in terms of the light-cone variables $u = t - r_*$ and $v = t + r_*$. We will apply the discretization scheme proposed in [10],

$$\Psi(N) = \Psi(W) + \Psi(E) - \Psi(S) - \Delta^2 V(S) \frac{\Psi(W) + \Psi(E)}{4} + \mathcal{O}(\Delta^4), \quad (3.2)$$

where the following notation for the points were used: $N \equiv (u + \Delta, v + \Delta)$, $W \equiv (u + \Delta, v)$, $E \equiv (u, v + \Delta)$, and $S \equiv (u, v)$. The Gaussian initial data are imposed on the two null surfaces, $u = u_0$ and $v = v_0$. Then, the dominant quasinormal frequencies can be extracted from the time-domain profiles with the help of the Prony method [17].

In the frequency domain we will use the WKB method of Will and Schutz [11], which was extended to higher orders in [12–14] and achieved even higher accuracy via using of the Padé approximants [14, 15]. The higher-order WKB formula has the following form [16],

$$\begin{aligned} \omega^2 = & V_0 + A_2(\mathcal{K}^2) + A_4(\mathcal{K}^2) + A_6(\mathcal{K}^2) + \dots \\ & - i\mathcal{K}\sqrt{-2V_2} (1 + A_3(\mathcal{K}^2) + A_5(\mathcal{K}^2) + A_7(\mathcal{K}^2) + \dots), \end{aligned} \quad (3.3)$$

where \mathcal{K} is half-integer. The corrections $A_k(\mathcal{K}^2)$ are of the order k to the eikonal formula and are polynomials in \mathcal{K}^2 with rational coefficients. The corrections $A_k(\mathcal{K}^2)$ depend on the values

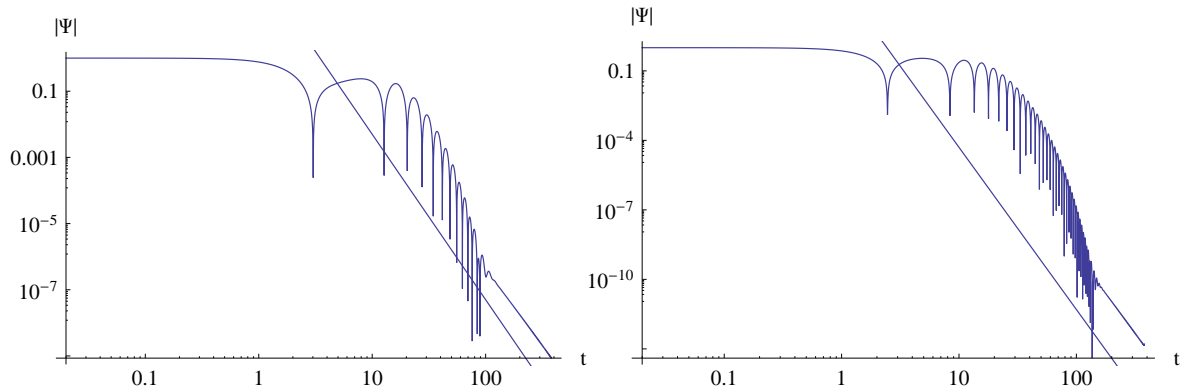


Figure 1. Logarithmic plots of late time tails for the electromagnetic radiation at $\ell = 1$ (left) and $\ell = 2$ right. The decay law is $|\Psi| \sim t^{-2\ell-3}$.

of higher derivatives of the potential $V(r)$ in its maximum. In order to increase accuracy of the WKB formula, we will follow Matyjasek and Opala [14] and use the Padé approximants. Here we will use the sixth order WKB method with $\tilde{m} = 5$, where \tilde{m} is defined in [14, 16], because this choice provides the best accuracy in the Schwarzschild limit and concordance with the time-domain integration.

Since both the WKB and time-domain integration methods are extensively used and discussed in the literature (see, for example, reviews [8, 16]), we will not describe them in this paper, but will simply show that both methods are in a good agreement in the common parametric range of applicability.

From Tables (1, 1) we see that the larger is the ratio a_0/M at a fixed mass of the black hole, that is, the more rarefied is the environment, the closer quasinormal frequencies to their Schwarzschild values. For the best fitting of the galaxies, this occurs at $a_0 \gtrsim 10^4 M$ in which case the difference with the Schwarzschild value is a small fraction of one percent. When a_0/M is decreased, both real oscillation frequencies and damping rates are decreased, while their ratio $Re(\omega)/Im(\omega)$, characterising the quality factor of the oscillations is slightly increased, which, quite counter-intuitively, makes the black hole a better oscillator when the galactic environment is taken into consideration.

The asymptotic tails for the perturbation are found via time-domain integration in the regime $M_{BH} \ll M \ll a_0$ and shown on fig. 1. There, one can see that the decay law, up to the numerical accuracy, is the same as that for the Schwarzschild case [18]

$$|\Psi| \sim t^{-2\ell-3}. \quad (3.4)$$

4 Grey-body factors

Calculation of grey-body factors are important, first of all for estimation of the portion of the initial radiation in the vicinity of the event horizon which is reflected back to it by the potential barrier. For this one have to find the reflection and transmission coefficients or solve the so called *scattering problem*, for which the boundary conditions are different from those required by quasinormal mode problem.

In the scattering problem we will consider the wave equation (2.2) with the boundary conditions allowing for incoming waves from infinity. Owing to the symmetry of the scattering

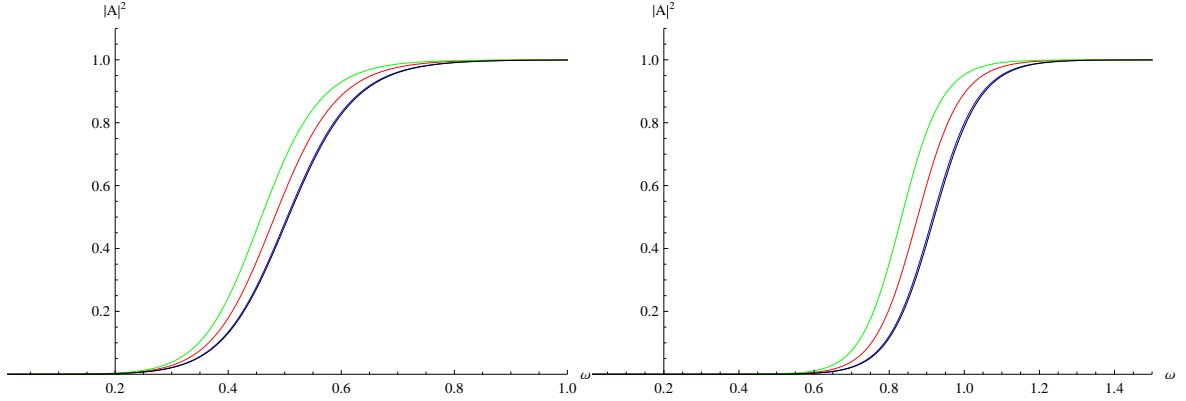


Figure 2. Grey body factors for the electromagnetic field $\ell = 1$ (left) and $\ell = 2$ (right), $M_{BH} = 1/2$, $M = 10M_{BH}$, $a_0 = 2000M$ (black), $a_0 = 200M$ (blue), $a_0 = 20M$ (red), $a_0 = 10M$ (green).

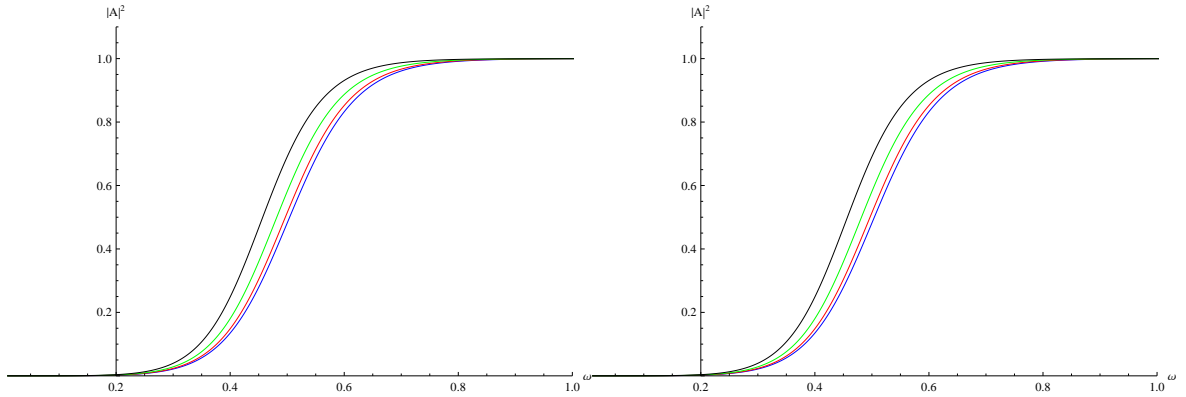


Figure 3. Grey body factors for the electromagnetic field $\ell = 1$ (left) and $\ell = 2$ (right), $M_{BH} = 1/2$, $a_0 = 1000M$, $M = 10M_{BH}$ (blue), $M = 40M_{BH}$ (red), $M = 100M_{BH}$ (green), $M = 200M_{BH}$ (black).

properties, this is identical to the scattering of a wave coming from the horizon. The scattering boundary conditions for (2.2) have the following form

$$\begin{aligned} \Psi &= e^{-i\omega r_*} + R e^{i\omega r_*}, & r_* \rightarrow +\infty, \\ \Psi &= T e^{-i\omega r_*}, & r_* \rightarrow -\infty, \end{aligned} \quad (4.1)$$

where R and T are the reflection and transmission coefficients.

The effective potential has the form of the potential barrier which monotonically decreases at both infinities, so that the WKB approach [11–13] can be applied for finding R and T . Since ω^2 is real, the first order WKB values for R and T will be real [11–13] and

$$|T|^2 + |R|^2 = 1. \quad (4.2)$$

Once the reflection coefficient is calculated, we can find the transmission coefficient for each multipole number ℓ

$$|\mathcal{A}_\ell|^2 = 1 - |R_\ell|^2 = |T_\ell|^2. \quad (4.3)$$

From fig. 2 we see that the smaller is the ratio a_0/M , the larger is the grey-body factors. In other words, the larger is the size of the halo under the same mass M , the bigger fraction of

radiation will be scattered back to the black hole. The latter can be easily understood, because the effective potential at smaller a_0/M becomes lower and, thereby, easier for transmission of radiation. If the size of the halo is fixed, but its mass is varied, then the larger mass leads to larger grey-body factors. However, as in the case of quasinormal modes, for $a_0 \sim 10^4 M$ the estimation differ from the Schwarzschild case insignificantly.

5 Unruh temperature

Here we would like to study the Unruh temperature of the spacetime under consideration, because this temperature is a characteristic of the surface gravity (or acceleration) experienced by an observer at a given distance from the black hole. This characteristic was also studied within alternative approaches to gravitational theory [19] (see also [20] and references therein). In the general relativistic context one starts from a generalized form of the Newtonian potential

$$\phi = \frac{1}{2} \log(-g^{\alpha\beta} \xi_\alpha \xi_\beta), \quad (5.1)$$

where e^ϕ is the red-shift factor that is supposed to be equal to unity at the infinity ($\phi = 0$ at $r = \infty$), if the space-time is asymptotically flat. The background metric is supposed to be some static solution which admits a global time-like Killing vector ξ_α .

The acceleration is defined by the formula

$$a^\alpha = -g^{\alpha\beta} \nabla_\beta \phi, \quad (5.2)$$

and the Unruh temperature on the shell of a fixed radius is given by the formula

$$T = \frac{\hbar}{2\pi} e^\phi n^\alpha \nabla_\alpha \phi, \quad (5.3)$$

where n_α is a unit vector, that is normal to the holographic screen and the Killing time-like vector ξ_β . Using the equation (5.3), the Unruh temperature can be written in the form

$$T = \frac{\hbar}{2\pi} e^\phi \sqrt{g^{\alpha\beta} \phi_{,\alpha} \phi_{,\beta}} = \frac{\hbar}{4\pi} \frac{f'(r)}{\sqrt{f(r) \left(1 - \frac{2m(r)}{r}\right)}} \quad (5.4)$$

From fig. ?? we see that larger values of mass of the halo M result in a smaller surface gravity, while for larger ratio of a_0/M this is not so: at smaller distance, large values of a_0/M (i.e. more rarified environment) corresponds to larger surface gravity while in the far region this is not so, and larger a_0/M correspond to smaller surface gravity.

At the event horizon $r_H = 2M_{BH}$ the Unruh temperature goes over into the Hawking temperature

$$T_H = \frac{\sqrt{\exp\left(-\sqrt{\frac{M}{2a_0 - M + 4M_{BH}}}\left(\pi - 2 \tan^{-1}\left(\frac{a_0 - M + 2M_{BH}}{\sqrt{M(2a_0 - M + 4M_{BH})}}\right)\right)\right)}}{8\pi M_{BH}}$$

When a_0 is large the Hawking temperature of the black hole horizon is

$$T_H \approx \frac{a_0 - M}{8\pi a_0 M_{BH}},$$

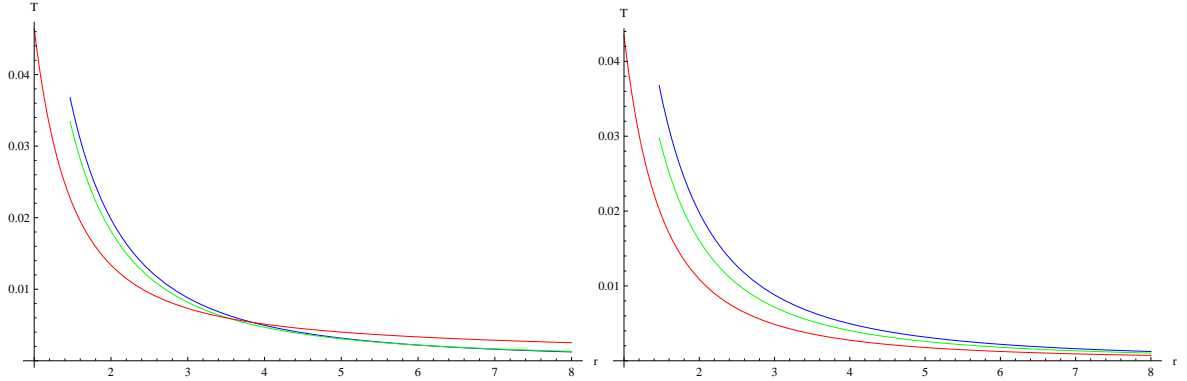


Figure 4. The Unruh temperature as a function of radial coordinate for various values of a_0 (left) and M (right). Right panel: $a_0 = 1000$, $M = 10M_{BH}$ (blue), $M = 400M_{BH}$, $M = 1000M_{BH}$ (red). Left panel: $M = 10M_{BH}$, $a_0 = 2000M_{BH}$ (blue), $a_0 = 100M_{BH}$ (green), $a_0 = 20M_{BH}$ (red)

approaching the Schwarzschild value in the limit $M \rightarrow 0$. Unlike the Unruh temperature at given r as a characteristic of acceleration or surface gravity, this expression for Hawking temperature must be interpreted carefully, as, evidently, we cannot claim that the black hole is in a kind of thermal equilibrium with the whole galaxy and practically the thermodynamic equilibrium is established in a relatively small region near the black hole.

6 Conclusions

Here we studied quasinormal modes, asymptotic late time tails and scattering properties of the electromagnetic radiation in the background of a black hole immersed in the Hernquist-type density distribution. Estimations made in the regime which is best fitting the galaxies behavior show that influence of the environment on radiation phenomena around such black holes must be relatively small.

Acknowledgments

I acknowledge support of the grant 19-03950S of Czech Science Foundation (GAČR).

References

- [1] V. Cardoso, K. Destounis, F. Duque, R. P. Macedo and A. Maselli, [arXiv:2109.00005 [gr-qc]].
- [2] M. Visser, Phys. Rev. D **46** (1992), 2445-2451 [arXiv:hep-th/9203057 [hep-th]].
- [3] J. Bamber, O. J. Tattersall, K. Clough and P. G. Ferreira, Phys. Rev. D **103** (2021) no.12, 124013 [arXiv:2103.00026 [gr-qc]].
- [4] P. T. Leung, Y. T. Liu, W. M. Suen, C. Y. Tam and K. Young, Phys. Rev. Lett. **78** (1997), 2894-2897 [arXiv:gr-qc/9903031 [gr-qc]].
- [5] R. A. Konoplya, Phys. Lett. B **795** (2019), 1-6 [arXiv:1905.00064 [gr-qc]].
- [6] R. A. Konoplya, Z. Stuchlík and A. Zhidenko, Phys. Rev. D **99** (2019) no.2, 024007 doi:10.1103/PhysRevD.99.024007 [arXiv:1810.01295 [gr-qc]].
- [7] L. Hernquist, Astrophys. J. **356** (1990), 359

- [8] R. A. Konoplya and A. Zhidenko, *Rev. Mod. Phys.* **83**, 793-836 (2011) [arXiv:1102.4014 [gr-qc]].
- [9] K. D. Kokkotas and B. G. Schmidt, *Living Rev. Rel.* **2**, 2 (1999) [gr-qc/9909058].
- [10] C. Gundlach, R. H. Price and J. Pullin, *Phys. Rev. D* **49**, 883 (1994) [gr-qc/9307009]
- [11] B. F. Schutz and C. M. Will, *Astrophys. J.* **291**, L33 (1985).
- [12] S. Iyer and C. M. Will, *Phys. Rev. D* **35**, 3621 (1987).
- [13] R. A. Konoplya, *Phys. Rev. D* **68**, 024018 (2003) [gr-qc/0303052].
- [14] J. Matyjasek and M. Opala, *Phys. Rev. D* **96**, no. 2, 024011 (2017) [arXiv:1704.00361 [gr-qc]].
- [15] Y. Hatsuda, arXiv:1906.07232 [gr-qc].
- [16] R. A. Konoplya, A. Zhidenko and A. F. Zinhailo, *Class. Quant. Grav.* **36**, 155002 (2019) [arXiv:1904.10333 [gr-qc]].
- [17] Hauer, J.F.; Demeure, C.J.; Scharf, L.L. (1990). "Initial results in Prony analysis of power system response signals". *IEEE Transactions on Power Systems*. 5: 80–89.
- [18] R. H. Price, *Phys. Rev. D* **5** (1972), 2439-2454 doi:10.1103/PhysRevD.5.2439
- [19] E. P. Verlinde, *JHEP* **04** (2011), 029 doi:10.1007/JHEP04(2011)029 [arXiv:1001.0785 [hep-th]].
- [20] R. A. Konoplya, *Eur. Phys. J. C* **69** (2010), 555-562 [arXiv:1002.2818 [hep-th]].